Progress In Electromagnetics Research Letters, Vol. 20, 119–128, 2011

HIGH POWER VHF FREQUENCY-HOPPING FILTERS WITH HIGH SUPPRESSION OF SECOND HARMONIC

Z.-Y. Zhao, P.-H. Li, K.-L. Cheng, and W.-Q. Cao

Institute of Communications and Engineering
PLA University of Science and Technology
2 Biaoying at YuDao Street, Nan Jing, Jiangsu 210007, China

K.-H. Chen

The 63rd Research Institute of the PLA GSH
18 Houbiaoying Road, Nan Jing, Jiangsu 210007, China

Abstract—A compact helix structure implementation and associated design formula of lumped element second-order bandpass filter circuit for high power frequency-hopping (FH) filter are proposed in this paper. The filter schematic provides one, two or three finite transmission zeros (Tzs), and these Tzs locate in the upper stopband to improve the rejection of stopband above the center frequency, especially the suppression of second harmonic with two Tzs. The filter is built on a common grounded helix coil of inductive coupled resonator tanks whose suspectance is tunable. Due to the parasitical capacitance of the helix coil, the filter has a feedback capacitor between input and output. Its working mechanism is revealed both mathematically and graphically. The measured results have a good agreement with the 3D full-wave electromagnetic simulation responses. The experimental filter has an insertion loss < 1.2 dB, a return loss > 15 dB, a 3-dB bandwidth of $5.8\% \sim 8.3\%$ over entire operating range with the power handling capability greater than 49 dBm and the suppression of second harmonic better than 66 dB.

Received 20 December 2010, Accepted 21 January 2011, Scheduled 27 January 2011
Corresponding author: Zhi-Yuan Zhao (zhaozhiyuan1998@163.com).

1. INTRODUCTION

FH filters are often used in multiband telecommunication systems, radiometers, and wideband radar systems, and typically based on different technologies such as: 1) mechanically tuning [1, 2]; 2) barium strontium titanate (BST) thin film technology [3]; 3) yttrium-iron-garnet(YIG)-based resonators [4]; 4) RF micro-electro-mechanical systems (RF-MEMS) devices [5]; 5) semiconductor (silicon, ferroelectric, GaAs) varactors [6, 7]; 6) LC elements [8]. However, none of the approaches can meet the requirement of VHF FH filters with high power handling capability and high linearity. In [9] and [10], the tunable filters are digitally controlled by the PIN diodes with capacitor array, thus the technique can meet the requirement of high speed in the FH radio system.

As the transmitter terminal filter and frond-end pre-election filter, FH filter's performance affects the whole system directly which can improve the anti-jamming capability of communications system and the sensitivity of receiver. The FH filter behind power amplifier can reject transmitting noise and spurious, thus it can improve SNR than traditional lowpass filter. Low power digital FH filter is already studied and applied a lot, however high power handling capability ($P_1\,\mathrm{dB} > 47\,\mathrm{dBm}$) FH filter is few reported, so the research is important and meaningful.

The modern VHF communications system requires filters with low loss and high Q. The helical filters have a high Q ($200 \sim 5000$), and wide operating frequency range ($10\,\mathrm{MHz} \sim 1200\,\mathrm{MHz}$) [11], thus it can transmit the HF and VHF signals of power between 50 W to 100 W. Zhao and Liang proposed the helical resonator which was loaded in the middle of the helix and the tuning element of COMS switch was set outside the cavity. Broad tuning range was realized and it was suitable for HF radio system [12].

In this paper, a compact helix structure is proposed with Tzs introduced by the coupling between input and output. The parasitical capacitance of the helix coil has been used exactly to enhance the suppression of second harmonic. The emphasis of this paper is also placed on revealing the working mechanism of the FH filter schematic both mathematically and graphically. The graphic solution suggests that the locations of the Tzs (one, two, or three zeros cases are discussed). As long as they are not too close to the center frequency, they do not change the pass-band characteristics of the filter too much. The design is co-simulated in CST MICROWAVE STUDIO and CST DC STUDIO. The inside size of the overall structure is $90*40*60\,\mathrm{mm}^3$.

2. THEORY

2.1. Theory on Electronically Tunable Filters

Designing a $[f_{0L}, f_{0H}]$ electronically tunable bandpass filter should obey the following rules: $f_{0L} = 30\,\text{MHz}$, $f_{0H} = 88\,\text{MHz}$, $f_0/f_{0L} = f_{0H}/f_0 = q$, $f_0 \approx 51\,\text{MHz}$, assuming that the capacitor $C_1 = C_2 = C_{12}$ (Fig. 1(a)) is corresponding to the center frequency f_0, C_{11} corresponding to the center frequency f_{0L}, C_{13} corresponding to the center frequency f_{0H}, according to $f = {1}\Big/{2\pi\sqrt{LC}}$, then $C_{12}/C_{13} = C_{11}/C_{12} = q^2 = 2.9$, the filter schematic should meet (1):

$$\begin{cases} 10\log|S_{11}(f_{0L})||_{C_1=C_2=C_{11}} < -15\,\text{dB}, \\ 10\log|S_{11}(f_{0H})||_{C_1=C_2=C_{13}} < -15\,\text{dB} \end{cases} \tag{1}$$

2.2. Theory of Chebyshev-type Filter with Tzs

The schematic of proposed filter to be implemented is shown in Fig. 1(a). It consists of a second-order bandpass filter with two lumped tunable capacitors (C_1 and C_2) in parallel with a feedback capacitor. The T-type inductor network plays the role of coupling and resonance. The feedback capacitor C introduces Tzs because of its coupling between input and output.

Assuming the admittance matrix for the filter schematic without C is $\mathbf{Y}' = \begin{pmatrix} y'_{11} & y'_{12} \\ y'_{21} & y'_{22} \end{pmatrix}$, the overall admittance matrix $\mathbf{Y}$ will be the sum of $\mathbf{Y}'$ and the admittance matrix for feedback C.

$$\mathbf{Y} = \begin{pmatrix} sC + y'_{11} & -sC + y'_{12} \\ -sC + y'_{21} & sC + y'_{22} \end{pmatrix} \tag{2}$$

where $s = j\omega$, the location of the finite Tzs can then be obtained by solving the following equation:

$$-sC + y'_{12} = 0 \tag{3}$$

To simply the analysis, the circuit in Fig. 1(a) is first transformed to the one shown in Fig. 1(b) using $T-\pi$ network transformation. The values of the inductors in this new configuration are given by

$$\begin{cases} M = L_{11} + L_{21} + \dfrac{L_{11}L_{21}}{L_0} & \text{(4a)} \\ L'_{11} = \dfrac{ML_0}{L_{21}} & \text{(4b)} \\ L'_{12} = \dfrac{ML_0}{L_{11}} & \text{(4c)} \end{cases}$$

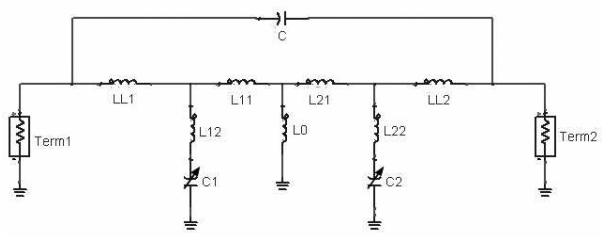

(a)

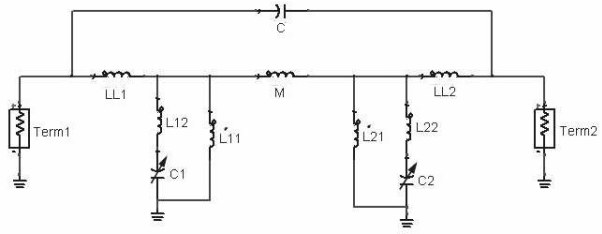

(b)

Figure 1. (a) Schematic of second-order filter. (b) Alternative representation of the filter schematic.

and then, by solving the nodal analysis on the circuit of the new schematic, the element y'_{12} can be found as:

$$y'_{12} = -\frac{1/LL_1LL_2M}{s^3\left[\left(\frac{sC_1}{s^2L_{12}C_1+1}+\frac{1}{sL'_1}\right)\left(\frac{sC_2}{s^2L_{22}C_2+1}+\frac{1}{sL'_2}\right)-\frac{1}{s^2M^2}\right]} \tag{5}$$

where $L'_1 = L'_{11}//LL_1//M$, $L'_2 = L'_{21}//LL_2//M$.

Substituting (5) into (3) and rewriting it as:

$$\begin{aligned} &s^6CC_1C_2\left(1+\frac{L_{12}L_{22}}{L'_1L'_2}+\frac{L_{12}}{L'_1}+\frac{L_{22}}{L'_2}-\frac{L_{12}L_{22}}{M^2}\right)\\ &+s^4\left[\frac{(L_{12}C_1+L_{22}C_2+L'_1C_1+L'_2C_2)C}{L'_1L'_2}\right.\\ &\left.-\frac{(L_{12}C_1+L_{22}C_2)C}{M^2}+\frac{L_{12}L_{22}C_1C_2}{LL_1LL_2M}\right]\\ &+s^2\frac{L_{12}C_1+L_{22}C_2}{LL_1LL_2M}+\frac{1}{LL_1LL_2M}=0 \end{aligned} \tag{6}$$

Because the filter schematic is synchronous and symmetrical, according to (5), the transmission function without C has one transmission zero, and its location is fixed by the product of L_{12} (or L_{22}) and C_1 (or C_2), namely $f_{tz} = 1/2\pi\sqrt{L_{12}C_1}$.

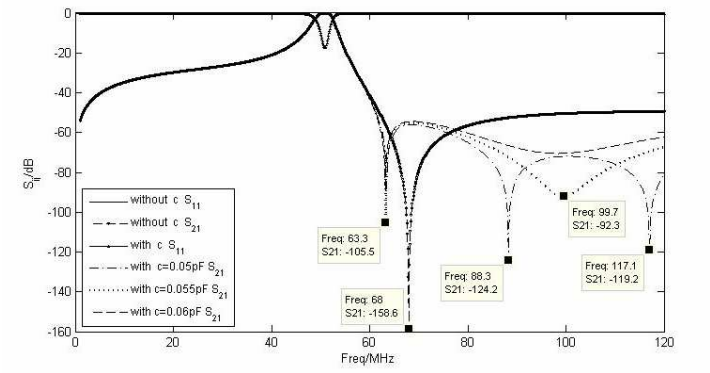

(a)

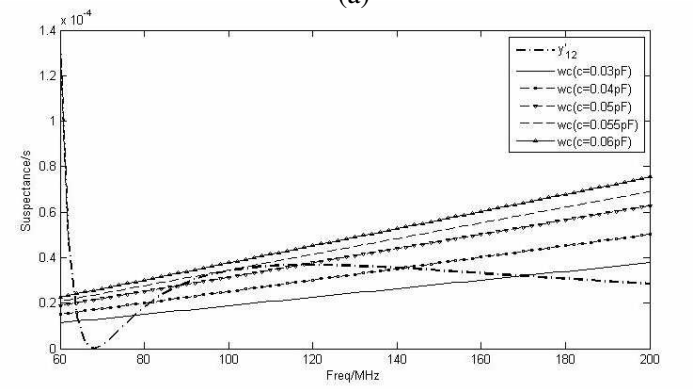

(b)

Figure 2. (a) S parameters of $f_0 = 51\,\text{MHz}$ and the locations of Tzs. (b) Locations of Tzs by method of graph.

According to the roots of (6), three cases may occur by choosing different feedback capacitor, shown in Fig. 2(a). These cases all can improve the selectivity. a. Three zeros locate above the center frequency, for example $C = 0.05\,\text{pF}$, this case has high rejection for the upper stopband overall but not second harmonic specifically. b. Two zeros locate above the center frequency, for example $C = 0.055\,\text{pF}$, this case has high suppression of second harmonic. c. One zero above the center frequency closer, for example $C = 0.06\,\text{pF}$, this case can improve the selectivity but the rejection will not be high enough. The roots of (3) and (5) are the Tzs' locations, as shown in Fig. 2(a). Conveniently, they can also be found by method of graph, as shown in Fig. 2(b), five lines corresponding to five suspectance of different capacitor cut the curve of suspectance of y'_{12}, so the intersections are the locations of Tzs.

2.3. Simulation of Circuit Model

Based on the synthesis method for a bandpass filter outlined in [1], a second-order Chebyshev-type bandpass filter of 5%-FBW, 0.01-dB ripple, whose element values for lowpass prototype are $g_0 = 1, g_1 = 0.4489, g_2 = 0.4078, g_3 = 1.1008$, 51 MHz center frequency, has been designed. The coupling coefficient of Resonators is extracted in the way of [13] by adjusting the common grounded helix coil, and the tapped position of input and output match network is found by 3D EM simulation according to the designing formula (7).

$$\begin{cases} k_{12} = \frac{FBW}{\sqrt{g_1 g_2}} \\ Q_{e1} = \frac{g_0 g_1}{FBW}, \quad Q_{e2} = \frac{g_2 g_3}{FBW} \end{cases} \tag{7}$$

where, k_{12} is coupling coefficient and Q_{e1}, Q_{e2} are external quality factors. The corresponding component values in Fig. 1(b) are $LL_1 = LL_2 = 195\,\text{nH}$, $L_{12} = L_{22} = 63\,\text{nH}$, $L'_{11} = L'_{21} = 67\,\text{nH}$, $M = 456.6\,\text{nH}$, $C_1 = C_2 = 87\,\text{pF}$.

In Fig. 2(a), the long dashed curve with the triangle mark shows the transmission response without feedback capacitor of the Chebyshev-type bandpass filter with one transmission zero itself. For highest suppression of second harmonic, the feedback capacitor must be chosen reasonably to produce a transmission zero near 102 MHz. Fig. 2(b) shows that the line of ωC is tangent with the curve of y'_{12} fitly, and transmission response is the short dashed curve in Fig. 2(a).

3. HELICAL FILTER IMPLEMENTATION

To actualize $M = 456.6\,\text{nH}$, according to (4a), L_0 must be very small, the grounded transmission line can satisfy, $L_0 = \frac{Z_0 \tan \beta l}{\omega}$ (Z_0 is the character impedance, and β is phase constant).

According above, the parasitical capacitance of the helix coil is needed to design exactly to improve the suppression of second harmonic. The parasitical capacitance formula of helix coil in [14] is $C_P = \frac{0.0295}{\log_{10}(1.2\,\text{S/d})}\,\text{pF/mm}$ (S is width of cavity, d is diameter of helix coil). The parameters of the whole common grounded helix coil are as follows: wire diameter is 2.2 mm, number of turns is 8, diameter of form is 15.2 mm, length of form is 50.4 mm, but the helix coil is not well-proportioned at the tapped position. The topology structure of FH filter is shown in Fig. 3(a), and experimental prototype is shown in Fig. 3(b).

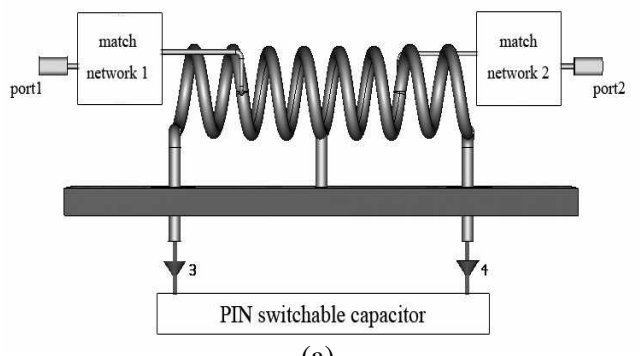

(a)

(b)

Figure 3. (a) The topology structure of FH filter. (b) Experimental prototype.

4. EXPERIMENTAL RESULTS AND DISCUSSION

In experiment, the common grounded inductor is the manual helix coil of high Q, and the capacitors of the 100 B serials of ATC are chosen as the capacitor array, and the PIN diodes of the MA4Pxxx serials of MA/COM are chosen as the switches. Using programmable logic device (PLD), the digital circuits of FH filter produce low or high voltage to control the PIN diodes forward or reverse bias, then select different capacitors combining with resonance circuit to accomplish different operating frequency filter characteristic. At last, the 3D EM simulation and experiment results are shown in Fig. 4.

In lower frequency, there are some burs attributed to the capacitances of the PIN off-switches. The more off-switches, the more burs occur. The FBWS and locations of the Tzs deviate from the predefined cases a little due to the error between theoretic inductance

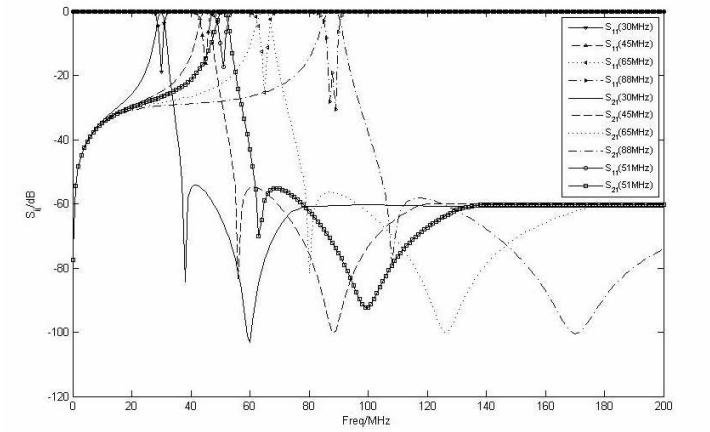

(a)

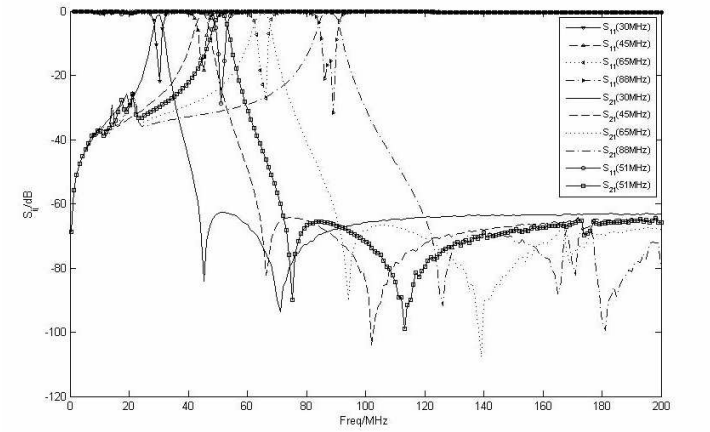

(b)

Figure 4. (a) Transmission and reflection response of the CST simulation. (b) Transmission and reflection response of the experiment.

and manual helix coil. The input power of the filter is greater than 49 dBm, and the output power is greater than 47 dBm when the filter is put in the surroundings of high and low temperature. The experimental results of different center frequencies are compared in Table 1. The filter has an insertion loss (I. L.) less than 1.2 dB, shape factor (BW_{30dB}/BW_{3dB}) less than 8 and suppression of second harmonic better than 66dB over operation frequency range from 30 MHz to 88 MHz.

Table 1. Comparison of experimental results.

f_0 (MHz)	I. L. (dB)	FBW_{3dB}	BW_{30dB} /BW_{3dB}	Tzs (MHz)	Suppression of $2f_0$ (dB)
30	1.02	8.3%	5.7	45.2, 71.2	66.5
45	1.05	7.8%	7.1	66.2, 102.2	70.4
51	0.82	5.8%	7.5	75.2, 113.1	73.8
65	0.94	6.7%	7.6	94.2, 139.1	77.8
88	0.97	6.8%	7.8	126.1, 181	67.9

5. CONCLUSION

In this paper, a compact helix second-order FH filter with high power handling capability is presented. The structure and the theory are proposed in detail, and the method of choosing the feedback capacitor for highest suppression of second harmonic is revealed. ADS and CST softwares are used to build up, simulate and optimize the model for the digital FH filter. The results of experiment are almost according with the simulation. The center I. L. and the suppression of second harmonic are fine.

REFERENCES

1. Hong, J.-S. and M. J. Lancaster, *Microstrip Filters for RF/Microwave Applications*, Wiley-Interscience, New York, 2001.
2. Abunjaileh, A. I. and I. C. Hunter, "Tunable combline bandstop filter with constant bandwidth," *IEEE MTT-S Dig.*, 1349–1352, June 2009.
3. Zhang, K., T. Watson, A. Cardona, and M. Fink, "$BaSrTiO_3$-based 30–88 MHz tunable filter," *IEEE MTT-S Dig.*, 1942–1945, May 2010.
4. Qiu, G., C. S. Tsai, B. S. T. Wang, et al., "A YIG/GGG GaAs-based magnetically tunable wideband microwave band-pass filter using cascaded band stop filters," *IEEE Transactions on Magnetics*, Vol. 44, No. 11, 3123–3126, November 2008.
5. Hall C. A., R. C. Luetzelschwab, R. D. Streeter, et al., "A 25 watt RF MEM-tuned VHF bandpass filter," *IEEE MTT-S Dig.*, 503–506, June 2003.
6. Brown, A. R., "A varactor tuned RF filter," *IEEE Transactions on Microwave Theory and Technique*, 1–4, October 1999.
7. Xozyrev, A., A. Ivanov, V. Keis, et al., "Ferroelectric films

nonlinear properties and applications in microwave devices," *IEEE MTT-S Dig.*, 985–988, June 1998.

8. Bouhamame, M., S. Amiot, O. Crand, et al., "Integrated tunable RF filter for TV reception," *ICECS*, Vol. 14, 837–840, December 2007.
9. Chen, Kunhe, Z. Chen, and L. Zhu, "Design of a high power digital tunable filter," *Proc. ICMMT*, Vol. 7, 496–498, May 2010.
10. Chen, J.-X., J. Shi, Z.-H. Bao, and Q. Xue, "Tunable and switchable bandpass filters using slot-line resonators," *Progress In Electromagnetics Research*, Vol. 111, 25–41,2011.
11. Vander Hagen, G. A., "The electrical tuning of helical resonators," *Microwave Journal*, Vol. 10, No. 8, 84–90, November 1967.
12. Zhao, L. and C. Liang, "Study of the HF electronically tunable power filter," *CAS Symp. IEEE Emerging Technologies: Mobile and Wireless Comm.*, Vol. 6, 303–304, May 2004.
13. Tyurnev, V. V., "Coupling coefficients of resonators in microwave filter theory," *Progress In Electromagnetics Research B*, Vol. 21, 47–67, 2010.
14. Zverev, A. I. and H. J. Blinchikoff, "Realization of a filter with helical components," *IRE Transactions on Component Parts*, Vol. 9, 99–110, September 1961.